Real-time current sensor fault detection and localization in DFIG wind turbine systems

Hamza Touioui, Abderahmane Ganouche, Zahir Ahmida, Hacene Bouzekri, Fouad Tachi
Department of Electrical Engineering, University of 20 August 1955, Skikda, Algeria

Article Info

ABSTRACT

The degree of reliability is one of the main issues in having the uninterrupted operation of fault-tolerant measurement and control systems. This paper presents a technique for detecting and localizing current sensor fault in doubly fed induction generator wind turbine systems (DFIG-WT). For this purpose, a methodology divided into three steps has been carried out and is presented as follows: the first step is the application of the zero-sequence component as an indicator of the presence of the sensor fault. The second step is based on the application of Concordia transformation on the current signals to generate different criteria for localizing the faulty sensor. Finally, an artificial neural network model is developed to analyze the localization criteria and identify the faulty sensor. All simulations are carried out in MATLAB/Simulink environment. Results show that the proposed technique is effective and can be used in real-time fault detection and localization in the DFIG-WT.
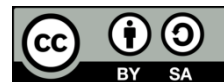
Corresponding Author:

Hamza Touioui
Department of Electrical Engineering, Faculty of Technology, University of 20 August 1955
Aissa Boukerma, G11 building N°04, Skikda, Algeria
Email: h.touioui@univ-skikda.dz

1. INTRODUCTION

The DFIG associated with the AC/DC/AC converter is one of the essential components usually deployed in sizeable grid-connected wind turbines due to their ability to provide power at constant voltage and frequency while the rotor speed varies, which allows better wind capture compared to fixed-speed wind turbines. However, DFIG-WT is overly sensitive to unknown grid inputs, such as disturbances, noises, and sensor faults [1], [2].

Fault detection and diagnosis in real-time operating mode of DFIG-WT are essential to the operation and management of automated systems [3]. There is a strong need to develop diagnostic systems capable of autonomously detecting the presence of anomalies and localizing faults that may occur in various components of DFIG-WT during operation [4]. Due to their ability to handle non-linearities in complex systems more efficiently and their benefits in real-time applications, ANNs have become increasingly crucial in fault detection and diagnosis. Therefore, designing ANN models for fault detection in wind turbines is advantageous [5], [6].

Diagnostic systems use sensor readings to assess the system's state, detect abnormal conditions, and determine the root cause to recommend corrective actions to operators to prevent significant system damage [7]. Sensors are considered the monitoring interface for dynamic systems because measurement data is the only source of information about the system. They are designed to generate reliable measurement data that provide estimates of variables or parameters.

Under certain operating conditions, unanticipated inconsistencies between sensor readings and their expected values can immediately lead to the instability of the system being monitored. Identifying the source of the failure is critical for monitoring systems because different corrective actions or compensatory responses are required in the event of a sensor or system failure, depending on the diagnostic decision. Much research has been done in fault detection to extract sensor faults from measurement data [7]. This work aims to develop a method for detecting and localizing current sensor faults in DFIG-WT. To this end, a technique based on zero-sequence component is used for current sensor fault detection because of its fast data processing speed. The technique is non-invasive, simple, and does not require complex calculations [8], [9].

A two-dimensional representation based on the Concordia current vector is performed by transforming a three-phase system (I_a, I_b, and I_c) into a two-phase system ($I_{\alpha n}$, $I_{\beta n}$) in different ways [10], [11]; this reduces the number of current components and makes the computation easier [12], [13]. From the expressions $I_{\alpha n}$ and $I_{\beta n}$, we define three localization criteria (C_{r1}, C_{r2}, and C_{r3}) to isolate the faulty sensor. Each localization criterion is derived from only two measurements, so it is only sensitive to these two measurements and does not vary when the third sensor is faulty.

Concordia's transformation approach must be combined with intelligent techniques that automate fault detection and diagnosis [12], [14]. A feedforward backpropagation neural network (FF-BPNN) is used to analyze the localization criteria and determine the faulty sensor [15], [16]. In sim power system, Simulink is used to analyze and test the different performances of the DFIG-WT. The modeling and simulation of the DFIG-WT with the vector control technique are done on the MATLAB/Simulink platform.

This paper presents a current sensor fault detection method based on the zero-sequence component and a feedforward backpropagation neural network that uses the localization criteria as inputs to determine the faulty sensor localization. The paper is organized as follows: section 2 presents and explains the method used for this study. Section 3 shows and describes the results obtained from the detection and validation of the ANN model and the fault localization test in all possible operating cases. Finally, section 4 concludes the paper.

2. METHOD

This study employs combined techniques to detect and localize current sensor faults. To detect current sensor faults, the current signals I_a, I_b, and I_c are measured, then the absolute value of the zero sequence component of these measured currents is calculated, and finally, this value is compared to a predetermined threshold. The detection of the presence of the current sensor fault allows the localization process to start identifying the faulty sensor using an ANN model powered by localization criteria obtained from the Concordia transformation on the measured currents. The details of the method are presented in the sub-sections below and summarized in the flowchart in Figure 1.
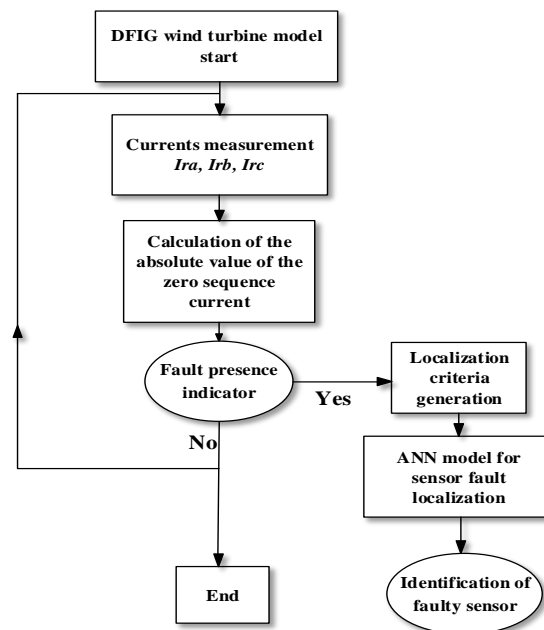

Figure 1. Flowchart of current sensor fault detection and localization

2.1. DFIG wind turbine system configuration

This section briefly describes the DFIG-WT architecture under study. The system considered for detection and localization has been developed in the MATLAB/Simulink environment, as shown in Figure 2. The designed system includes a generator connected directly to the grid on the stator side. The DFIG rotor circuit is supplied by a voltage source inverter controlled by a hybrid hysteresis current (HC) with field-oriented control (FOC) [17], [18].

In this system, a fixed hysteresis band is applied for the current control of the rotor side converter (RSC). As shown in Figure 3, hysteresis current control is basically a feedback current control technique [19], [20]. A hypothetical control band surrounding the reference current controls the current error, which is the difference between the reference and inverter currents [21]. When the load current exceeds the upper band, the comparator output is activated so that the output voltage is altered to decrease the load current and maintain it between the bands; it is deactivated when the load current falls below the lower limit. The switching frequency varies with the distance between the upper and lower bands. The switching strategy is as [22]: $if\ i_{ra} > i_{ra}^*$ +HB, then upper switch is turned ON and $if\ i_{ra} < i_{ra}^*$ –HB, then lower switch is turned ON.
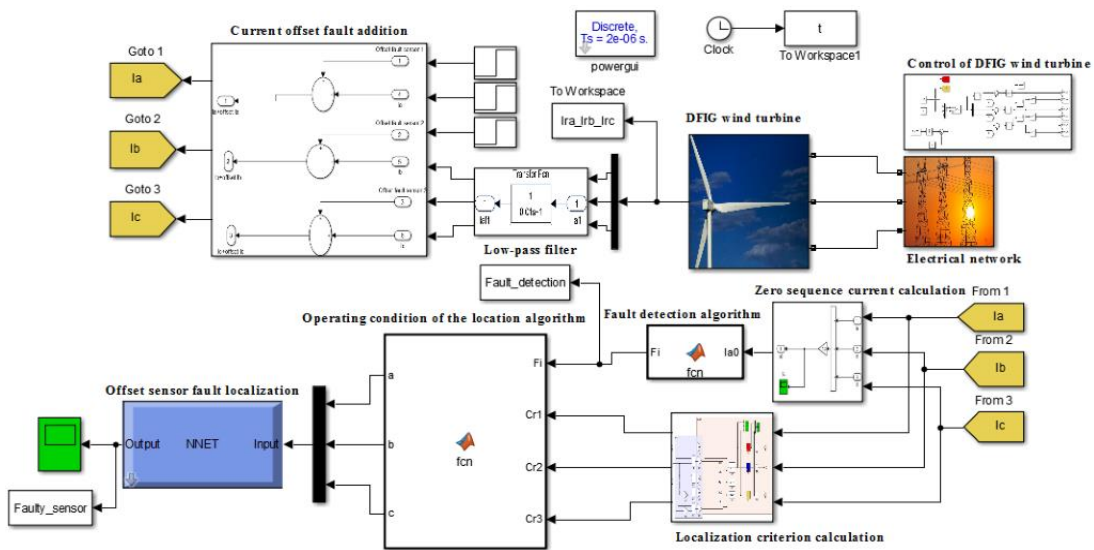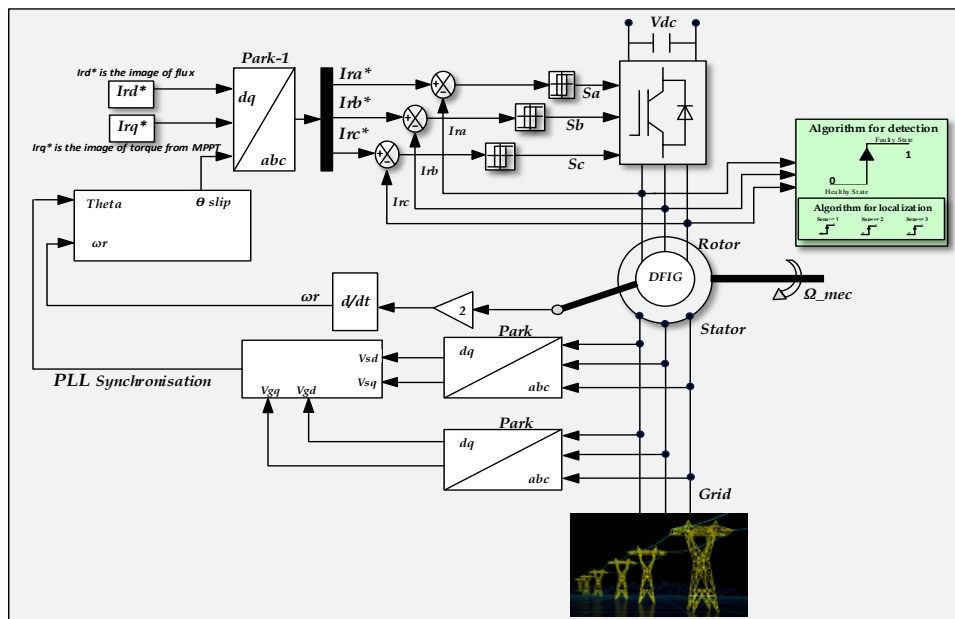

Figure 2. The simulated model of the system

Figure 3. Control block of rotor side converter

2.2. Current sensor faults detection using zero-sequence component

Due to their simplicity of implementation and the fact that they do not require complex calculations such as FFT, the zero-sequence component methods are widely used in online and real-time monitoring systems [8], [9]. In fact, in a double-fed induction generator, the connection to the grid does not usually use a neutral connection. Therefore, the grid current has no zero-sequence component, and the sum of the three-phase currents is zero [10], [23].

$$I_{a0} = \frac{1}{3}(I_a + I_b + I_c) \tag{1}$$

$$abs\,(I_{a0}) \approx 0 \tag{2}$$

For healthy operation, the zero-sequence component of the measured current must be very small, almost zero, so that a fault in one of the current sensors can be detected [23]. A comparator can then be used to find out if one of the current sensors might be faulty. For this purpose, the absolute value of the measured zero-sequence current I_{a0} is compared to a current threshold I_{th}. Consequently, when a fault occurs in one of the current sensors, the output of this comparator, denoted F_i, becomes equal to 1. The choice of the current threshold I_{th} depends on the current sensor's accuracy [24], [25]. So, the detection can be done immediately whenever the zero-sequence current appears due to a sensor fault.

2.3. The Concordia transformation for the generation of fault localization criteria

In the previous sub-section, we defined the indicator F_i as an indicator of the presence of a fault, but it does not allow us to determine the localization of the faulty sensor. In order to generate fault localization criteria, an algorithm based on the Concordia transformation is applied as follows: if we have three current signals, I_a, I_b, and I_c, constituting a balanced three-phase system, we can calculate the Concordia transform in different ways [10], as given in Table 1.

Table 1. Calculation of the Concordia transformation by different ways

Expressions of the component on the α axis	Expressions of the component on the β axis
$I_{\alpha 1} = \sqrt{\frac{3}{2}}I_a$	$I_{\beta 1} = \sqrt{\frac{1}{2}}(I_b - I_c)$
$I_{\alpha 2} = -\sqrt{\frac{3}{2}}(I_b + I_c)$	$I_{\beta 2} = \sqrt{\frac{1}{2}}(I_a + 2I_b)$
	$I_{\beta 3} = -\sqrt{\frac{1}{2}}(I_a + 2I_c)$

The current component $I_{\alpha 1}$ can be calculated only using the measurement of the current in phase a (see $I_{\alpha 1}$ in Table1), whereas $I_{\alpha 2}$ is estimated using the measurement of the currents in phases b and c (see $I_{\alpha 2}$ in Table 1). Therefore, some α and β components might not be expressed in terms of the faulty current sensor. We define three localization criteria from these different expressions to isolate the faulty sensor. Each localization criterion is calculated from only two measurements, as shown in (3), (4), and (5). Therefore, it will only be sensitive to those two measurements and will not show any variation when the third sensor becomes faulty, as shown in Table 2.

$$C_{r1} = \left(I_{\alpha 2}^2 - I_{\beta 1}^2\right) \tag{3}$$

$$C_{r2} = \left(I_{\alpha 1}^2 - I_{\beta 3}^2\right) \tag{4}$$

$$C_{r3} = \left(I_{\alpha 1}^2 - I_{\beta 2}^2\right) \tag{5}$$

In a healthy system, Cr1, Cr2, and Cr3 exhibit nearly identical values. However, significant deviations arise when a sensor malfunctions, unless the same fault occurs simultaneously across all three sensors, which is highly unlikely. The localization criteria obtained by combining the coefficients α_n and β_n represent the input data of the ANN model, which has been trained for the various operating conditions to precisely determine the localization of the faulty sensor by an output set to "0" or "1".

Table 2. Sensitivity of the criteria to the current

Localization criteria	I_a	I_b	I_c	Used component
C_{r1}	-	+	+	$I_{\alpha 2}$, $I_{\beta 1}$
C_{r2}	+	-	+	$I_{\alpha 1}$, $I_{\beta 3}$
C_{r3}	+	+	-	$I_{\alpha 1}$, $I_{\beta 2}$

2.4. ANN sensor fault localization

In this work, a model developed using an FF-BPNN was applied to localize the faulty sensor in DFIG-WT. A three-layer nonlinear model has been trained using the Levenberg Marquardt algorithm to localize the faulty sensor [5], [26]. Four operating conditions were considered: healthy, fault at sensor 1, fault at sensor 2, and fault at sensor 3. As shown in Figure 4, the structure of the ANN fault locator was chosen as follows: 3 inputs, 1 hidden layer with 10 neurons, and 3 outputs.
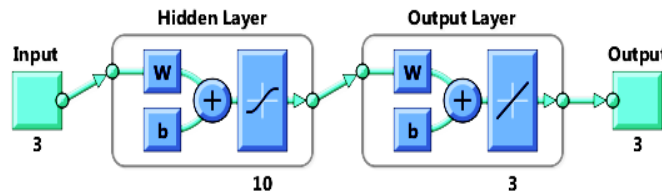

Figure 4. ANN training model

The inputs of the ANN fault locator are C_{r1}, C_{r2}, and C_{r3}, which are obtained from the Concordia coefficients (α_n, β_n) combination. The outputs of the locator are set to '0' or '1' depending on the state of each sensor according to the fault condition [27], as shown in Table 3. In order to ensure that the testing and validation process was rigorous and thorough, the ANN fault locator was tested and validated with different current sensor faults (gain and offset) to replicate the types of faults that can occur in real-world applications.

Table 3. Target output for ANN fault localization

Stat of sensors	Sensor 1	Sensor 2	Sensor 3
Healthy	0	0	0
Fault at sensor 1	1	0	0
Fault at sensor 2	0	1	0
Fault at sensor 3	0	0	1

3. RESULTS AND DISCUSSION

In this section, we will examine an offset fault, as illustrated in Figure 5. The offset fault is introduced in the Matlab simulation environment at 0.1 sec. To simulate this fault, a constant (known as the offset fault) is added to the output of the current Ia. This approach has been widely used in previous studies [28]–[30] to analyze the effects of offset faults in various systems. By considering this fault scenario, we can gain valuable insights into the behavior of the system and assess its robustness in the presence of such faults.

3.1. Results for detection

Figures 6(a) and 6(b) show the sensor current offset fault results. Figure 6(a) shows the zero-sequence current I_{a0} for both sensor operating conditions: healthy and faulty. On the other hand, Figure 6(b) represents the sensor fault presence indicator F_i by comparing the value I_{a0} with the zero-sequence current threshold I_{th}. The result contains two operating cases: healthy case '0' and faulty case '1'.

The most striking results that emerge from the data are the considerable increase in zero-sequence current in the presence of a current sensor fault and the speed of fault detection. Indeed, as illustrated in Figures 6(a) and 6(b), the value of I_{a0} is very low, nearly equal to zero, for the healthy case, and it varies significantly when a sensor fault occurs. Thus, the indicator F_i changes simultaneously from the healthy to the faulty state when the sensor fault occurs.
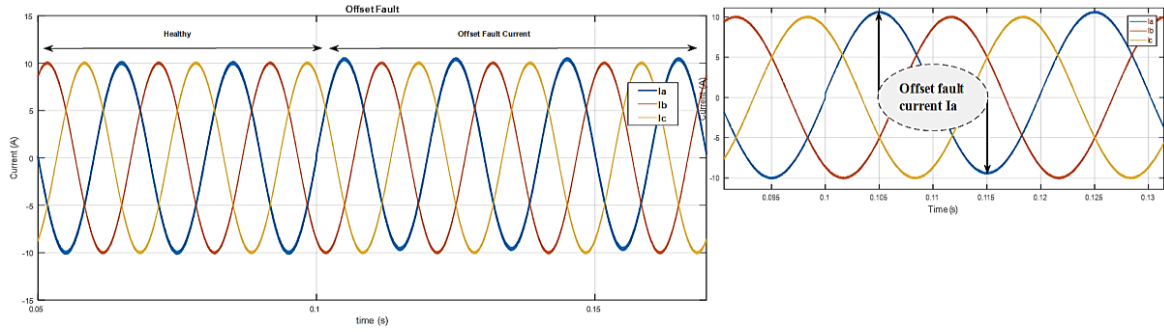
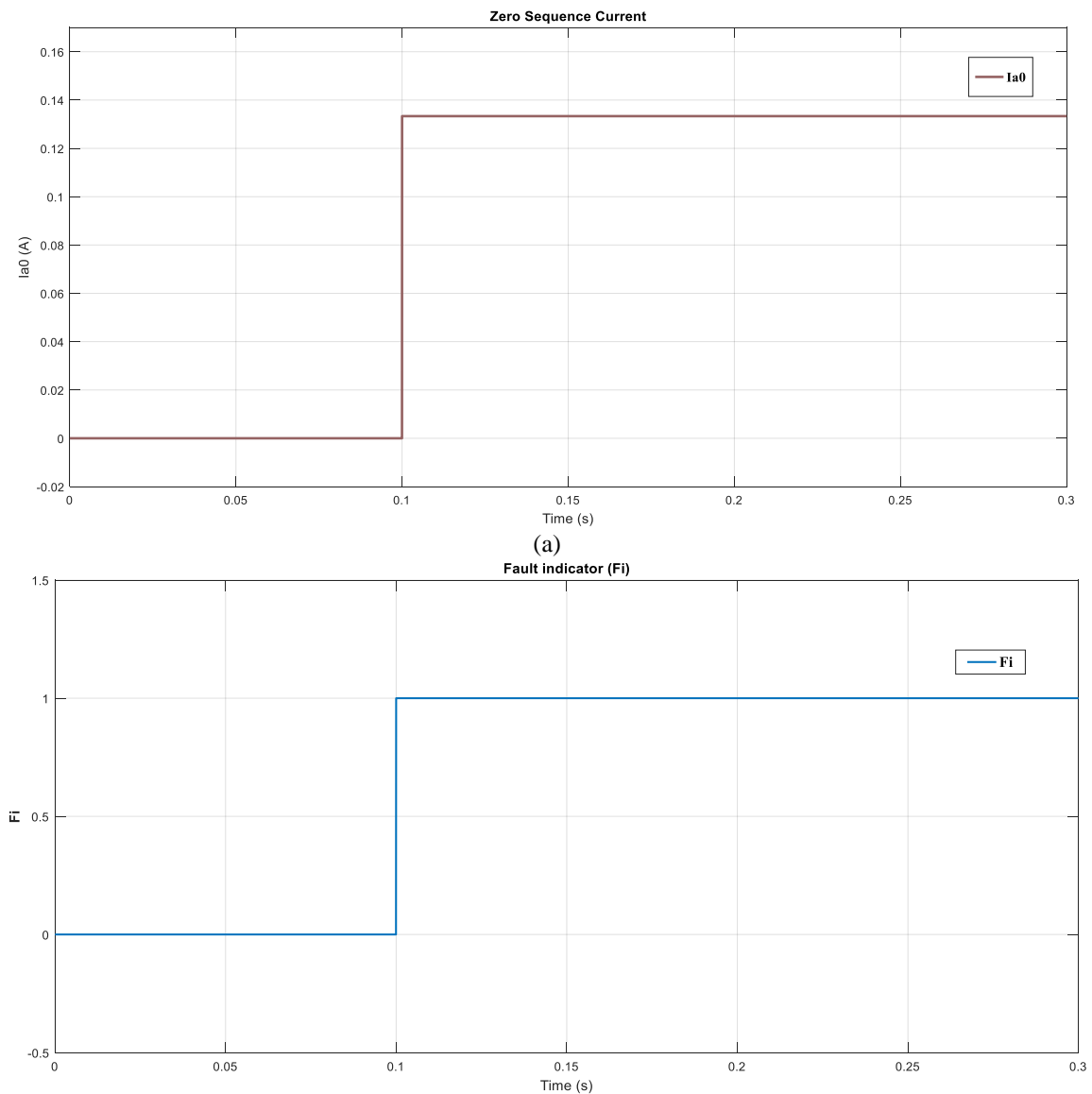Figure 5. The current sensors offset fault at t = 0.1(s)

(a)

Figure 6. Sensor current offset fault: (a) zero sequence current and (b) sensor fault presence indicator

3.2. Results for ANN training model

During the training process, the learning performance of the ANN model was evaluated by comparing the model's target and output using the learning regression plot. The learning process was

repeated until the performance results became satisfactory. The post-training performance plots are shown in Figures 7 and 8.
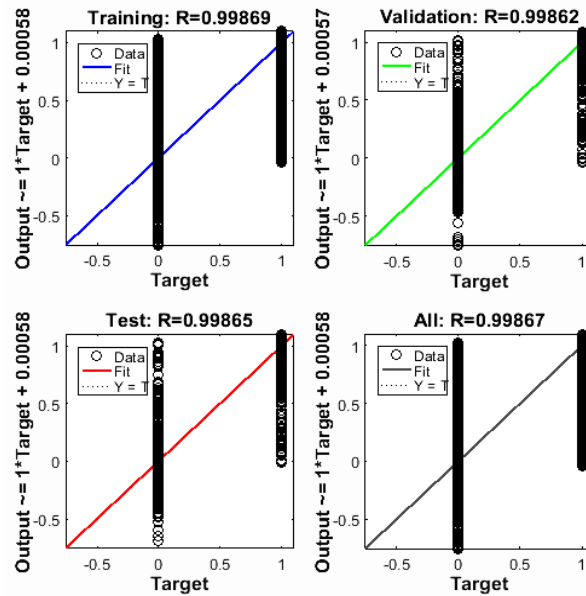
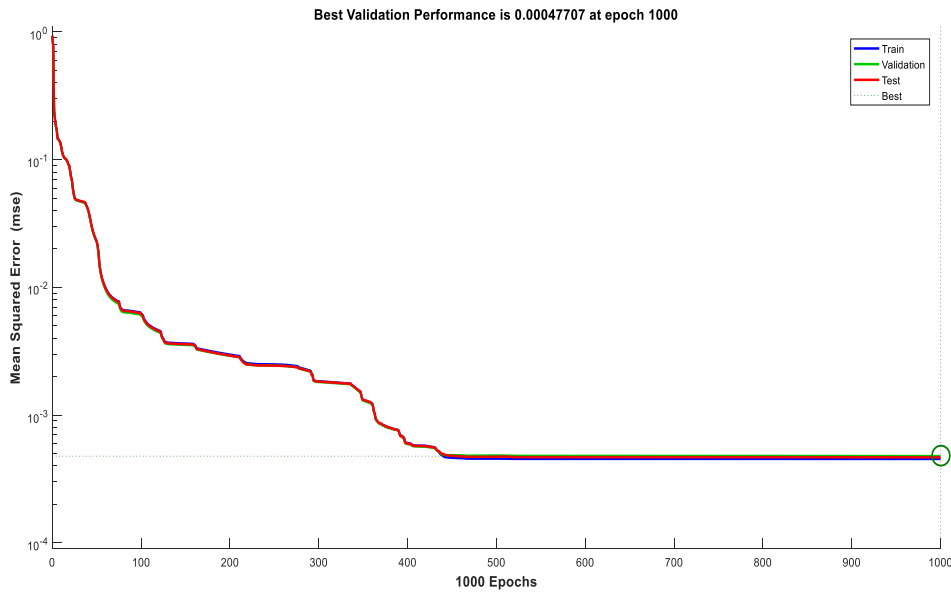Figure 7. Regression FIT of the output vs targets for the network

Figure 8. Mean squared error for training, validation and test

The correlation coefficient was found to be 0.99867 from Figure 7, which indicates a satisfactory correlation between the targets and the outputs. Thus, the results of mean-square error training, validation, and test plots in Figure 8 are feasible because of the similarity between the test curve and the validation curve and the nihility of the overfitting.

3.3. Results for sensor fault localization

The neural network model proposed here should localize the faulty sensor, as shown in Table 3 of the previous sub-section. The results obtained from the ANN fault localization model are presented in Table 4. The localization process has two possible cases for each of the three sensors: the healthy case, represented by '0',

and the faulty case, represented by '1'. Figure 9 shows an offset fault in sensor 1 (phase a) localized by the ANN localization model. It can be noticed from the data in Table 4 and Figure 9 that the ANN fault localization followed the target output for all operating conditions, and the test of faulty sensor localization showed good performance and efficiency.

The obtained results for fault detection, the learning process, and the localization of the faulty sensor indicate that the proposed method can detect and locate faulty current sensors with high accuracy and reliability. Furthermore, this method can detect current sensor faults early before they cause severe damage or downtime, which is a significant benefit. These advantages are achieved due to the small ANN structure, which makes it more efficient and faster than complex networks. In terms of fault detection, this can be important for real-time processing and decision-making. In conclusion, the proposed fault detection and localization method for faulty current sensors represents a significant improvement over existing techniques.

Table 4. Results of validation for ANN fault localization model

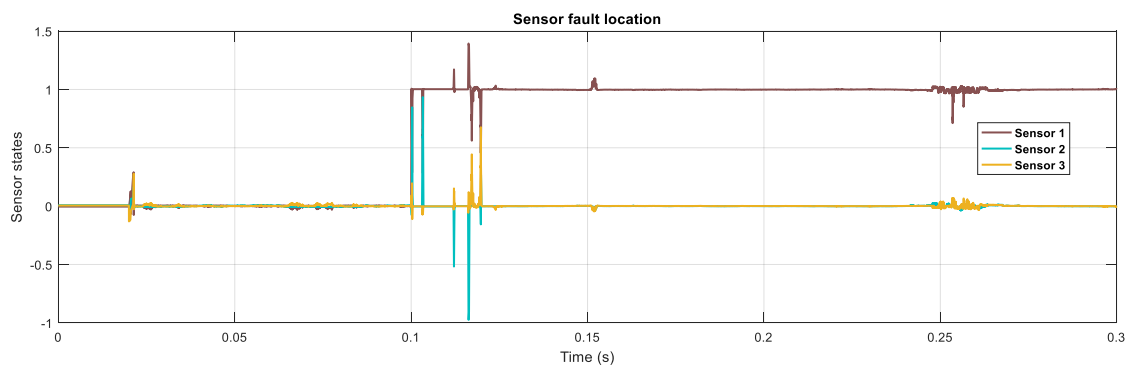| Condition	Target			ANN output		
	X	Y	Z	X	Y	Z
Healthy	0	0	0	9,43e-05	9,43e-05	9,43e-05
Fault at sensor 1	1	0	0	0,9998	0,0062	0,0019
	1	0	0	1,0016	0,0063	0,0036
	1	0	0	1,0031	0,0065	0,0052
Fault at sensor 2	0	1	0	-0,0018	1,0014	0,0024
	0	1	0	-0,0018	1,0014	0,0024
	0	1	0	-0,0018	1,0014	0,0024
Fault at sensor 3	0	0	1	0,0002	-0,0007	0,9991
	0	0	1	0,0002	-0,0007	0,9991
	0	0	1	0,0002	-0,0007	0,9991

Figure 9. Sensor offset fault localization

4. CONCLUSION

This paper presents the detection and localization current sensor faults in DFIG-WT using various techniques. Current sensor faults can be detected by a comparator that analyzes the current threshold of the zero-sequence component in DFIG-WT with isolated neutral load topology. However, a locator based on the FF-BPNN with the Levenberg Marquardt algorithm is developed to localize the faulty sensor. The primary benefit of the suggested method is its ease of implementation, and it does not involve many complex calculations. The proposed current sensor fault detection technique was found to have satisfactory performance. Thus, the obtained results showed that the ANN fault locator accurately tracked the target output for different data under all operating conditions. In conclusion, the developed detection and localization approach is a better candidate for online and real-time surveillance. Future research should focus on adding speed sensor faults to DFIG-WT systems and implementing a complete detection and localization algorithm in an extensive online and real-time monitoring system.

REFERENCES

[1]   F. Amrane, A. Chaiba, B. Francois, and B. Babes, "Real time implementation of grid-connection control using robust PLL for WECS in variable speed DFIG-based on HCC," *2017 5th International Conference on Electrical Engineering - Boumerdes, ICEE-B 2017*, vol. 2017-January, pp. 1–5, 2017, doi: 10.1109/ICEE-B.2017.8191984.
[2]   S. Kharoubi and L. El Menzhi, "Diagnosing multiple short circuit switches faults in wind turbine doubly-fed induction generator," *International Journal of Power Electronics and Drive Systems*, vol. 13, no. 1, pp. 547–553, 2022, doi: 10.11591/ijpeds.v13.i1.pp547-553.

[3] Y. Nyanteh, C. Edrington, S. Srivastava, and D. Cartes, "Application of artificial intelligence to real-time fault detection in permanent-magnet synchronous machines," *IEEE Transactions on Industry Applications*, vol. 49, no. 3, pp. 1205–1214, 2013, doi: 10.1109/TIA.2013.2253081.

[4] M. Taiebat and F. Sassani, "Distinguishing Sensor Faults From System Faults By Utilizing Minimum Sensor Redundancy," *Transactions of the Canadian Society for Mechanical Engineering*, vol. 41, no. 3, pp. 469–487, 2017, doi: 10.1139/tcsme-2017-0033.

[5] A. G. Kavaz and B. Barutcu, "Fault detection of wind turbine sensors using artificial neural networks," *Journal of Sensors*, vol. 2018, 2018, doi: 10.1155/2018/5628429.

[6] A. P. Marugán, F. P. G. Márquez, J. M. P. Perez, and D. Ruiz-Hernández, "A survey of artificial neural network in wind energy systems," *Applied Energy*, vol. 228, pp. 1822–1836, 2018, doi: 10.1016/j.apenergy.2018.07.084.

[7] M. Taiebat, "Distinguishing Sensor and System Faults for Diagnostics and Monitoring," 2015.

[8] S. Grubic, J. M. Aller, B. Lu, and T. G. Habetler, "A survey on testing and monitoring methods for stator insulation systems of low-voltage induction machines focusing on turn insulation problems," *IEEE Transactions on Industrial Electronics*, vol. 55, no. 12, pp. 4127–4136, 2008, doi: 10.1109/TIE.2008.2004665.

[9] S. Bakhri, N. Ertugrul, and W. L. Soong, "Negative sequence current compensation for stator shorted turn detection in induction motors," *IECON Proceedings (Industrial Electronics Conference)*, pp. 1921–1926, 2012, doi: 10.1109/IECON.2012.6388908.

[10] I. Bahri, M. W. Naouar, I. Slama-Belkhodja, and E. Monmasson, "FPGA-based FDI of faulty current sensor in current controlled PWM converters," *EUROCON 2007 - The International Conference on Computer as a Tool*, pp. 1679–1686, 2007, doi: 10.1109/EURCON.2007.4400529.

[11] M. Frini, A. Soualhi, and M. El Badaoui, "Gear faults diagnosis based on the geometric indicators of electrical signals in three-phase induction motors," *Mechanism and Machine Theory*, vol. 138, pp. 1–15, 2019, doi: 10.1016/j.mechmachtheory.2019.03.030.

[12] I. Y. Önel and M. E. H. Benbouzid, "Induction motor bearing failure detection and diagnosis: Park and concordia transform approaches comparative study," *IEEE/ASME Transactions on Mechatronics*, vol. 13, no. 2, pp. 257–262, 2008, doi: 10.1109/TMECH.2008.918535.

[13] F. Zidani, M. E. H. Benbouzid, D. Diallo, and M. S. Naït-Saïd, "Induction Motor Stator Faults Diagnosis by a Current Concordia Pattern-Based Fuzzy Decision System," *IEEE Transactions on Energy Conversion*, vol. 18, no. 4, pp. 469–475, 2003, doi: 10.1109/TEC.2003.815832.

[14] D. Diallo, M. E. H. Benbouzid, D. Hamad, and X. Pierre, "Fault detection and diagnosis in an induction machine drive: A pattern recognition approach based on concordia stator mean current vector," *IEEE Transactions on Energy Conversion*, vol. 20, no. 3, pp. 512–519, 2005, doi: 10.1109/TEC.2005.847961.

[15] M. Dybkowski and K. Klimkowski, "Artificial neural network application for current sensors fault detection in the vector controlled induction motor drive," *Sensors (Switzerland)*, vol. 19, no. 3, 2019, doi: 10.3390/s19030571.

[16] G. Jager *et al.*, "Assessing neural networks for sensor fault detection," *CIVEMSA 2014 - 2014 IEEE Conference on Computational Intelligence and Virtual Environments for Measurement Systems and Applications, Proceedings*, pp. 70–75, 2014, doi: 10.1109/CIVEMSA.2014.6841441.

[17] F. Amrane, A. Chaiba, B. E. Babes, and S. Mekhilef, "Design and implementation of high performance field oriented control for grid-connected doubly fed induction generator via hysteresis rotor current controller," *Revue Roumaine des Sciences Techniques Serie Electrotechnique et Energetique*, vol. 61, no. 4, pp. 319–324, 2016.

[18] F. Amrane, A. Chaiba, B. Francois, and B. Babes, "Experimental design of stand-alone field oriented control for WECS in variable speed DFIG-based on hysteresis current controller," *2017 15th International Conference on Electrical Machines, Drives and Power Systems, ELMA 2017 - Proceedings*, pp. 304–308, 2017, doi: 10.1109/ELMA.2017.7955453.

[19] M. H. N. Talib, S. N. M. Isa, H. E. Hamidon, Z. Ibrahim, and Z. Rasin, "Hysteresis current control of induction motor drives using dSPACE DSP controller," *PECON 2016 - 2016 IEEE 6th International Conference on Power and Energy, Conference Proceeding*, pp. 522–527, 2017, doi: 10.1109/PECON.2016.7951617.

[20] R. P. Aguilera, P. Acuna, G. Konstantinou, S. Vazquez, and J. I. Leon, "Basic Control Principles in Power Electronics: Analog and Digital Control Design," *Control of Power Electronic Converters and Systems*, 2018, doi: 10.1016/B978-0-12-805245-7.00002-0.

[21] S. R. Subbanna and M. Suryakalavathi, "Performance comparison between Hysteresis Controller (HC) and Proportional Integral (PI) Controller for Resistance Spot Welding System," *International Journal of Scientific & Engineering Research*, vol. 7, no. 11, pp. 768-774, 2016.

[22] E. M. Suhara and M. Nandakumar, "Analysis of hysteresis current control techniques for three phase PWM rectifiers," *2015 IEEE International Conference on Signal Processing, Informatics, Communication and Energy Systems, SPICES 2015*, 2015, doi: 10.1109/SPICES.2015.7091434.

[23] A. Duda and P. Drozdowski, "Induction motor fault diagnosis based on zero-sequence current analysis," *Energies*, vol. 13, no. 24, 2020, doi: 10.3390/en13246528.

[24] K. Rothenhagen and F. W. Fuchs, "Current sensor fault detection and reconfiguration for a doubly fed induction generator," *PESC Record - IEEE Annual Power Electronics Specialists Conference*, pp. 2732–2738, 2007, doi: 10.1109/PESC.2007.4342450.

[25] C. D. Tran, M. Kuchar, M. Sobek, V. Sotola, and B. H. Dinh, "Sensor Fault Diagnosis Method Based on Rotor Slip Applied to Induction Motor Drive," *Sensors*, vol. 22, no. 22, 2022, doi: 10.3390/s22228636.

[26] A. Adouni, D. Chariag, D. Diallo, M. Ben Hamed, and L. Sbita, "FDI based on Artificial Neural Network for Low-Voltage-Ride-Through in DFIG-based Wind Turbine," *ISA Transactions*, vol. 64, pp. 353–364, 2016, doi: 10.1016/j.isatra.2016.05.009.

[27] S. S. Moosavi, A. Djerdir, Y. Ait-Amirat, and D. A. Khaburi, "ANN based fault diagnosis of permanent magnet synchronous motor under stator winding shorted turn," *Electric Power Systems Research*, vol. 125, pp. 67–82, 2015, doi: 10.1016/j.epsr.2015.03.024.

[28] H. Tao, T. Peng, C. Yang, J. Gao, C. Yang, and W. Gui, "Voltage and Current Sensor Fault Diagnosis Method for Traction Converter with Two Stator Current Sensors," *Sensors*, vol. 22, no. 6, 2022, doi: 10.3390/s22062355.

[29] D. Diallo and C. Delpha, "Incipient offset current sensor fault detection and diagnosis using statistical analysis and the Kullback Leibler divergence for AC drive," *Proceedings IECON 2017 - 43rd Annual Conference of the IEEE Industrial Electronics Society*, vol. 2017-January, pp. 8070–8075, 2017, doi: 10.1109/IECON.2017.8217416.

[30] F. Grouz, L. Sbita, and M. Boussak, "Current sensors faults detection, isolation and control reconfiguration for PMSM drives," *2013 International Conference on Electrical Engineering and Software Applications, ICEESA 2013*, 2013, doi: 10.1109/ICEESA.2013.6578414.

BIOGRAPHIES OF AUTHORS

Hamza Touioui was born in Skikda, Algeria. He received the M.Sc. in electrical engineering from the University of Skikda, Algeria, in 2014. He is currently pursuing Ph.D. degree in Electrical Control and Industrial Systems at the Electrical Engineering department of the University of Skikda, Algeria. His main research interests are fault detection/diagnosis, renewable energy, motor drive, power system and control. He can be contacted at email: h.touioui@univ-skikda.dz.

Abderahmane Ganouche was born in Skikda, Algeria. He received the BSc, the MSc, and the PhD degrees from University of Skikda, Skikda, Algeria, in 2010, 2012, and 2018, respectively, all in Electrical Engineering. He is currently Lecturer in automatics engineering at the electrical engineering department, University of Skikda. His main research interests include modelling and control of wind energy conversion systems, advanced control theory and optimization. He can be contacted at email: a.ganouche@univ-skikda.dz.

Zahir Ahmida was born in Constantine, Algeria. He received the Ph.D. degree from the University Mentouri of Constantine, Algeria, in 2006. In 1988, he received the M.Sc. degree in Electronics Engineering from the University of Nottingham, United Kingdom. Currently, he is a Professor at the Electrical Engineering department of the University of Skikda, Algeria. His main research interests are control systems and signals, energy systems and cyber physical systems. He can be contacted at email: z.ahmida@univ-skikda.dz.

Hacene Bouzekri was born in Skikda, Algeria. He received the Ph.D. degree in electrical engineering from the Institut National Polytechnique Lorraine, France, in 1994. Currently, he is a research professor at the Electrical Engineering department of the University of Skikda, Algeria. He is head of the system modeling and control team at the Skikda Automation Laboratory (LAS). His main research interests are renewable energy, motor drive, power system and control. He can be contacted at email: habouzekri@gmail.com.

Fouad Tachi was born in Skikda, Algeria. received his State Engineer degree in Automatic Control from the Department of Electrical Engineering, University of Badji Mokhtar, Algeria, and the M.Sc. in Control Systems Engineering from the Department of Automatic Control and Systems Engineering, The University of Sheffield, U.K, in 1990 and 2004, respectively. He began his career as a Senior Instrumentation and Process Control instructor with Sonatrach/Algerian Petroleum Institute in 1990. In 1999, he moved to Sonatrach, where he was appointed Principal Instrumentation Engineer from 2006 to 2013. After that, he moved back to Sonatrach/Algerian Petroleum Institute, where he is currently a Lecturer/Researcher in Control Engineering. His research interests are systems modeling and identification, optimization, distributed control systems, intelligent systems, and fault diagnosis using machine learning and deep learning. He can be contacted at email: tfouad21@gmail.com.